DOI: 10.3727/105221618X15320123457380
GE-000582 Provisionally Accepted July 18, 2018 for publication in "Gene Expression: The Journal of Liver Research"

In *Atp7b-/-* Mice Modeling Wilson's Disease Liver Repopulation with Bone Marrow-derived Myofibroblasts or Inflammatory Cells and not Hepatocytes is Deleterious

Running title: Bone marrow transplantation in Wilson's disease

Yogeshwar Sharma[1], Jinghua Liu[2], Kathleen E. Kristian[3], Antonia Follenzi[4,5], and Sanjeev Gupta[1,4,6]

[1]Department of Medicine, Albert Einstein College of Medicine, Bronx, NY, USA; [2]Department of Obstetrics and Gynecology, Shanghai Public Health Clinical Center, Shanghai, China; [3]Department of Chemistry, Iona College, New Rochelle, NY, USA; [4]Department of Pathology, Albert Einstein College of Medicine, Bronx, NY, USA; [5]Department of Health Sciences, Università del Piemonte Orientale "A. Avogadro", Novara, Italy; and [6]Marion Bessin Liver Research Center, Diabetes Center, Cancer Center, and Ruth L. and David S. Gottesman Institute for Stem Cell and Regenerative Medicine Research, Albert Einstein College of Medicine, Bronx, NY, USA

¶Correspondence: Sanjeev Gupta, MD, Albert Einstein College of Medicine, Ullmann Building, Room 625, 1300 Morris Park Avenue, Bronx, NY 10461; Tel: 718 430 3309; Fax: 718 430 8975; e-mail: sanjeev.gupta@einstein.yu.edu.

Figures: 5

Tables: 2

Supplementary Material: No

Key Words: Copper, Cell therapy, Differentiation, Stem cells, Bone marrow transplantation

ABSTRACT

Background: In Wilson's disease, *ATP7B* mutations impair copper excretion with liver or brain damage. Healthy transplanted hepatocytes repopulate liver, excrete copper and reverse hepatic damage in animal models of Wilson's disease. In *Fah*-/- mice with tyrosinemia and alpha-1 antitrypsin mutant mice, liver disease is resolved by expansions of healthy hepatocytes derived from transplanted healthy bone marrow stem cells. This potential of stem cells has not been defined for Wilson's disease. **Methods:** In diseased *Atp7b*-/- mice we reconstituted bone marrow with donor cells expressing green fluorescent protein reporter from healthy transgenic mice. Mature hepatocytes originating from donor bone marrow were identified by immunostaining for green fluorescence protein and bile canalicular marker, dipeptidylpeptidase-4. Mesenchymal and inflammatory cell markers were used for other cells from donor bone marrow cells. Gene expression, liver tests and tissues were analyzed for outcomes in *Atp7b*-/- mice. **Results:** After bone marrow transplantation in *Atp7b*-/- mice, donor-derived hepatocytes containing bile canaliculi appeared within weeks. Despite this maturity, donor-derived hepatocytes neither divided nor expanded. Liver of *Atp7b*-/- mice was not repopulated by donor-derived hepatocytes: *Atp7b* mRNA remained undetectable; liver tests, copper content and fibrosis actually worsened. Restriction of proliferation in hepatocytes accompanied oxidative DNA damage. By contrast, donor-derived mesenchymal and inflammatory cells extensively proliferated. These contributed to fibrogenesis through greater expression of inflammatory cytokines. **Conclusion:** In Wilson's disease, donor bone marrow-derived cells underwent different fates: hepatocytes failed to proliferate; inflammatory cells proliferated to worsen disease

outcomes. This knowledge will help guide stem cell therapies for conditions with pro-inflammatory or pro-fibrogenic microenvironments.

INTRODUCTION

Physiologically-regulated gene expression could be restored by repopulating liver with healthy cells. This offers opportunities for therapeutics and translational models [1-6]. Liver conditions constitute multiple targets for cell therapy [7]. The potential of stem cell-derived lineages has been largely understood at gene expression levels [8; 9]. This may not accurately predict whether after transplantation cells will engraft and proliferate. As mature hepatocytes possess unique structures (gap junctions, bile canaliculi) [10; 11], this should allow alternative ways to determine fates of stem cells.

In *Fah*-/- mouse model of hereditary tyrosinemia, transplanted adult hepatocytes repopulate liver and correct disease [3; 4]. Hepatocytes originating from donor cells after bone marrow transplantation (BMT) exerted similar outcomes [3]. Also, in mice with mutant human alpha-1 antitrypsin, liver injury improved after intraportal transplantation of healthy BM-derived cells [12].

These stem cell therapies should be relevant for Wilson's disease (WD). Due to *ATP7B* mutations, hepatobiliary copper (Cu) excretion is deficient in WD. This causes serious liver and/or brain damage [13]. In animal models, biliary Cu excretion in WD may be restored by gene therapy or by transplanting healthy hepatocytes [14-16]. For instance, in LEC rats modeling hepatic WD, transplanted healthy hepatocytes repopulated liver with disease correction: *Atp7b* mRNA deficiency resolved; hepatic injury and fibrosis regressed[14; 15]. For transplanted hepatocytes to excrete Cu, reconstitution was necessary of bile canaliculi, This will be critical for treating WD with stem cells[17].

To determine the therapeutic potential of BM-derived hepatocytes, we used hepatic Cu toxicosis model of WD in *Atp7b-/-* mice [18]. As after intrahepatic transplantation, BM-derived nucleated cells were rapidly cleared from liver [19], we considered BM reconstitution will be better. After BMT, donor-derived stem cells should constantly appear in blood with recurrent opportunities for originating hepatocytes. In turn, these donor-derived hepatocytes should have proliferated as replacements for damaged and lost native hepatocytes.

MATERIALS AND METHODS

Animals: Animal Care and Use Committee of Albert Einstein College of Medicine approved protocols. Donor C57BL/6 mice were from National Cancer Institute (Bethesda, MD); transgenic C57BL/6-TgCAG-EGFP/1Osb/J mice expressing green fluorescent protein (GFP) were from Jackson Laboratories (Bar Harbor, ME). GFP+/- donors were used due to neurotoxicity in GFP+/+ mice. In GFP+/- mice 50% cells expressed GFP; correction factor of 2 was applied for donor-derived cells. *Atp7b-/-* mice were originally from S. Lutsenko. These were backcrossed 10 times into C57BL/6 background in Stem Cells, Animal Models and Cell Therapy Core. Animals received chow with 11.8 mg copper/kg (Ralston Purina, St. Louis, MO).

BMT: Femur and tibia were flushed by Dulbecco's Modified Eagle's Medium containing 5% fetal bovine serum (DMEM; Life Technologies, Carlsbad, CA) with RBC lysis as described [20]. *Atp7b-/-* mice of 6-7 weeks age, males and females in equal numbers, received total body irradiation (TBI) to 6 and 5 Gray in two sessions 3h apart. This was followed 8-10 x10^6 total BM cells in DMEM via tail vein. Death was not an end-point.

Hepatocyte transplantation: Donor GFP+ transgenic hepatocytes were isolated by collagenase perfusion [21]. Freshly isolated 1x10^6 hepatocytes in 0.1 ml DMEM were transplanted into 6-7 week-old *Atp7b-/-* mice (n=6) via spleen. Animals were sacrificed for liver repopulation analysis after 1mo and 3 mo.

GFP+ BM-derived cells and hepatocytes: Tissues were fixed in 4% paraformaldehyde in phosphate buffered saline, pH 7.4 (PAF) for 4h, immersed in 20% and 30% sucrose for 2h and 36h, respectively, embedded in optimal cooling temperature (OCT) resin, and stored at −80°C. Cryosections of 5μm were post-fixed with PAF and stained with rabbit anti-GFP (1:300, Molecular Probes, Life Technologies) using for detection either Alexa Fluor®488-conjugated goat anti-rabbit IgG (1:500, Cat#A-11008, Molecular Probes), as described [20], or goat anti-rabbit IgG, horseradish peroxidase conjugate (1:500, AP187P, Sigma-Aldrich, St. Louis, MO) with DAB+ Substrate-Chromogen (Dako Inc., Carpinteria, CA). For donor-derived Kupffer cells (KC), monocytes or mesenchymal cells, GFP staining was followed by F4/80 staining with phycoerythrin-conjugated antibody (1:100, Cat#MF48004, Caltag Labs, U.K.), or vimentin staining with Alexa Fluor-647-conjugated antibody (1:100, Cat#9856, Cell Signaling, MA). For donor-derived hepatocytes, GFP staining was followed by albumin staining with phycoerythrin-conjugated anti-rabbit goat IgG (1:100, Cat#T6778, Sigma-Aldrich). Dipeptidylpeptidase-4 (Dpp4) was stained with fluorescein isothiocynate-conjugated antibody (1:100, Cat#559652, BD Biosciences, San Diego, CA). Counterstaining used Fluorishield with DAPI (Cat#GTX30920 GeneTex, Irvine, CA). Morphometry used multiple tissue sections from several mice (n=3-4 each).

Liver histology and grading: Tissues were fixed in 10% buffered formalin for paraffin embedding and hematoxylin-eosin staining. Tissue grading included steatosis, polyploidy (megalocytes with enlarged nuclei containing >diploid DNA), apoptosis, and mitosis with maximal score of 13, as described [22].

Hepatic fibrosis: Collagen was stained by Sirius Red (Picrosirius Red Stain Kit, Cat#24901, Polysciences Inc., PA), Stained areas were quantitated under x400 magnification by ImageJ software (NCI, Bethesda, MD). Hydroxyproline was measured by a kit (MAK008, Sigma-Aldrich).

Hepatic DNA damage. Tissue sections were fixed with ethanol and treated with 250 ng/mL RNAse for 1h at 37ºC. DNA was denatured by 4M HCl for 7 min followed by neutralization with 50 mM Tris base for 2 min. Sections were blocked with 10% goat serum in PBS for 1h and incubated with 8-oxo-dG antibody (1:1000, Cat-4354-MC-050, Clone 2E2, Trevigen Inc, Gaithersburg, MD) overnight at room temperature. Detection used Alexa Fluor®647-conjugated goat anti-mouse IgG (1:100, Cat#4410, Cell Signaling, MA) for 1h with DAPI counterstaining.

Hepatic Cu content: Tissue samples, 2-5 mg in weight, were desiccated and solubilized in 10 mM nitric acid, as described previously [23]. Cu was measured by atomic absorption spectrometry with detection limit of 100 ng/g liver (Varian AA240, Varian Medical Systems, Palo Alto, CA).

Reverse transcription (RT)-PCR: Total RNA was extracted by TRIzol Reagent (Invitrogen Corp, Carlsbad, CA), cleaned with RNeasy and treated with DNase (Qiagen Corp, Valencia, CA). cDNA was prepared from 1µg of RNA with Omniscript RT Kit

(Qiagen Corp, Valencia, CA). PCR cycles for Atp7b and Gapdh were: denaturation at 94°C x 3 min; 30 cycles at 94°C x 30s, 60°C x 45s, 72°C x 45s; and 72°C x 7 min. PCR products were resolved in 2% agarose. Quantitative RT-PCR for fibrosis and inflammation-related genes used QuantiTect® SYBR® Green PCR kit (CAT# 204143, Qiagen) with triplicate samples per condition. PCR cycles were: denaturation at 95°C x 10 min; 40 cycles at 95°C x 15s, 60°C x 60s; and 72°C x 10 min. Primers are listed (**Table 1)**. Gene expression was normalized to *Gapdh*. Fold-differences used $2^{\Delta\Delta}$Ct method.

Serological tests: Samples were stored at -20°C. A commercial kit was used for serum alanine aminotransferase activity (ALT) (Cat#700260, Cayman Chemical, Ann Arbor, MI). Serum ceruloplasmin was measured as described [14]

Statistical analysis: Data are shown as means ± SEM. Differences were analyzed by t-tests or analysis of variance (ANOVA) with Kruskall-Wallis test by GraphPad Prism7 (Graph-Pad Software, La Jolla, CA). $P<0.05$ was considered significant.

RESULTS

With BMT, no fatality was observed over 2 weeks in *Atp7b-/-* mice. BM chimerism was >85%, as determined in randomly selected mice (n=5) by flow cytometry for GFP+ blood cells. This reproduced our experience with BMT protocol [20].

We established groups of healthy C57BL/6 and *Atp7b-/-* mice (**Fig. 1A**). To reveal BM-derived cells, we analyzed mice 3 mo after BMT (n=3), and found GFP+ cells (**Fig. 1B)**. These were mostly in hepatic sinusoids, i.e., KC or monocytes. GFP+ hepatocytes with large nuclei, abundant cytoplasm and albumin were infrequent (0-1 per section). Donor-derived hepatocytes displayed Dpp4+ bile canaliculi. When adult hepatocytes were

transplanted, cells engrafted next to portal areas. After 1mo, 2±3 transplanted hepatocytes were in each group. Transplanted hepatocytes after 3 mo constituted larger groups; 35±28 cells each, p<0.001. Thus, in *Atp7b-/-* mice healthy hepatocytes proliferated.

In untreated *Atp7b-/-* controls (n=40), 3 mice (7%) died spontaneously over 12 mo. In *Atp7b-/-* mice plus BMT (n=53), 27 mice (51%) died over 12 mo, p<0.001. No mortality was observed in healthy C57BL/6 mice.

Serum ALT in healthy C57BL/6 mice (n=4) was 54±17 u/L (**Fig. 1C**). ALT levels in untreated Atp7b-/- mice (n=8) were higher, 172±36 u/L, p<0.001. After BMT, ALT levels were higher still, after 6 mo (n=8) and 12 mo (n=4), 447±127 u/L and 214±110 u/L, respectively. Ceruloplasmin levels were lower in *Atp7b-/-* mice with or without BMT versus C57BL/6 controls (**Fig. 1D**).

Liver fibrosis accelerated in *Atp7b-/-* mice after BMT

Untreated *Atp7b-/-* mice showed multiple WD-associated changes. In *Atp7b-/-* mice with BMT, liver histology worsened (**Fig. 2A**). Megalocytosis marking advanced polyploidy was prominent after BMT. Sirius Red showed more fibrosis after BMT (**Fig. 2B**). Histological grading after 12 mo, was: 2±0, 6.3±0.3 and 7.9±0.3 in healthy C57BL/6 (n=9), untreated *Atp7b-/-* controls (n=8) and *Atp7b-/-* mice with BMT (n=7), respectively, p<0.001, ANOVA (**Fig. 2C**). Sirius Red area in healthy controls (n=9) was 8.7±0.9%, rising in *Atp7b-/-* mice (n=8) and *Atp7b-/-* mice with BMT (n=7) to 31.7±2.2% and 38.3±0.9%, respectively, p<0.001, ANOVA. Hepatic hydroxyproline increased from 0.2±0.1 mg/g in C57BL/6 mice (n=4) by 2.5-, 4.5- and 3.5-fold in *Atp7b-/-* controls or mice 6 mo and 12 mo after BMT (n=4 ea), respectively, p<0.001, ANOVA **(Fig. 2D**).

Hepatic Cu content, Atp7b mRNA expression and cell damage

Healthy C57BL/6 mice (n=9) had 0.016±0.00 mg Cu/g liver after 12 mo. In untreated *Atp7b-/-* controls (n=8), significantly more Cu was found, 0.18±0.01 mg/g, p<0.001. In *Atp7b-/-* mice with BMT, liver Cu was even higher, both after 6 mo (n=9) and 12mo (n=7), 0.26±0.05 mg/g and 0.38±0.05 mg/g, respectively, p<0.05 **(Fig. 3A)**. *Atp7b* mRNA was present in only healthy C57BL/6 mice and not untreated *Atp7b-/-* or *Atp7b-/-* mice with BMT (n=3 ea) **(Fig. 3B)**. This suggested donor-derived hepatocytes did not repopulate liver after BMT. To determine the basis for lack of proliferation in native hepatocytes, we examined oxidative DNA damage, which results from Cu toxicosis, and impairs liver regeneration [24] **(Fig. 3C)**. In healthy C57BL/6 mice, hepatic 8-oxo-dG adducts were not prominent. *Atp7b-/-* mice showed considerable 8-oxo-dG adducts, particularly in megalocytes or polyploid cells and also in inflammatory and stromal cells. This damage in native hepatocytes was more pronounced in *Atp7b-/-* mice with BMT. Losses of these cells should have led to greater compensatory proliferation in healthy donor-derived hepatocytes.

Inflammation and fibrosis-related genes were expressed more after BMT

Genes contributing to inflammation (*IL6, TNF-α*) and fibrogenesis (*TGF-β, MMP2, TIMP1 and COL1*) were expressed more in Atp7b-/- mice versus healthy controls (n=3 ea) **(Fig. 4)**. *IL6, TNF-α, and TGF-β* were expressed even more in *Atp7b-/-* mice after BMT (n=3) – more after 6 mo versus 12 mo - fibrotic tissue in latter samples could have affected gene expression. As inflammation likely recruited cell types aggravating fibrosis, *MMP2, TIMP1* and *COL1* expression profiles were in agreement with this possibility.

Replacement of liver cell types by donor BM-derived cells

Donor-derived GFP+/Dpp4+ hepatocytes were still surprisingly rare after 12 mo. In *Atp7b-/-* mice with BMT we observed neither proliferating donor-derived cells nor liver repopulation (**Fig. 5A**). GFP+ donor cells were mostly in hepatic sinusoids with F4/80+ monocytes or macrophages **(Fig. 5B)**. GFP+/vimentin+ mesenchymal cells, including myofibroblasts, were also abundant **(Fig. 5C)**.

Morphometry indicated donor-derived cell types 12 mo after BMT constituted Dpp4+ hepatocytes in <0.05%, F4/80+ monocytes/macrophages in 14%, and vimentin+ mesenchymal cells in 84% of the cases (**Table 2**).

DISCUSSION

Donor BM generated multiple cell types in Atp7b-/- mice, although hepatocytes were infrequent, which was similar to previous reports [3; 20]. Extensive BM chimerism along with numerous monocytes/macrophages indicated BMT was successful. The contribution of TBI for replacing native BM is critical. Although TBI may cause early inflammation and endothelial injury (later, veno-occlusive disease, VOD); after successful BMT, these complications abate or resolve. Long-term hepatic damage after TBI is limited - after one year mice exhibit only mitosis [25]. Alternatively, BMT may use drug myeloablation, e.g., busulfan and cyclophosphamide [26]. However, VOD may actually be more severe with these drugs, as opposed to TBI. That was not the case in our study.

In pluripotent stem cells, hepatic differentiation is restricted, at best, to early-stage fetal hepatocytes in vitro [9; 27]. Stem cell differentiation is aided by additional signals and cues in vivo. This differentiation is achieved by incompletely understood and complex mechanisms, including transcription factor regulation, protein-protein interactions, RNA-

protein changes, DNA methylation, epigenetic reprogramming, etc [27]. These mechanisms are difficult, if not impossible, to decipher in rare donor-derived cells in vivo.

Presence of Dpp4+ bile canaliculi in BM-derived hepatocytes indicated maturity [10; 11]. To date, no study has utilized this stringent marker in WD of Dpp4+ bile canaliculi for stem cell-derived hepatocytes. This structure-based analysis should be significant as gene expression alone to characterize cell maturity has often been inadequate [6; 8; 9]. Lack of hepatic *Atp7b* mRNA and continued Cu accumulation after BMT were prominent in our study. Histological abnormalities also worsened after BMT. This differed from toxic milk mouse model of Cu toxicosis, where transplantation of healthy BM in sublethally irradiated recipients decreased hepatic Cu [28]. The fate of transplanted BM-derived cells in that study was not evaluated. Also, it was unknown whether Cu was excreted in bile.

Proliferation restriction in BM-derived hepatocytes was another issue for therapeutic benefits. Inability of BM-derived hepatocytes to correct disease in *Atp7b*-/- mice concerned two major processes: 1) donor BM-derived hepatocytes with bile canaliculi were uncommon, and 2) proliferation in BM-derived hepatocytes was restricted. Anti-proliferative effects of Cu, potential growth factor deficiencies, ECM alterations, inflammation, or other changes were likely contributors.

A major difference in animal models of WD (*Atp7b*-/- mice) versus tyrosinemia (*Fah*-/- mice) is that Cu toxicosis causes intracellular injury plus extracellular perturbations due to tissue inflammation, fibrosis and ECM changes [14; 15]. In the *Fah*-/- state, toxic tyrosine metabolites are restricted to hepatocytes without such inflammation or fibrosis [29]. Similar considerations apply to mice with mutant alpha-1 antitrypsin and intracellular

injury [12]. We did not focus on whether BM-derived cells fused with native hepatocytes, as in *Fah*-/- mice [30]. This cell fusion had not interfered with disease correction [3].

In LEC rat model of WD, transplanted hepatocytes repopulate liver, and hepatic radiation or other pro-oxidant treatments, in fact, accelerates proliferation in transplanted hepatocytes [14; 15]. Similarly, healthy hepatocytes proliferated in *Atp7b-/-* mice. As Cu alters ECM to impair cell survival and/or proliferation [31], this might have affected donor-derived hepatocytes. Remote TBI should not have directly injured donor-derived hepatocytes. Hepatic radiation in excess of that after TBI did not exacerbate fibrosis in LEC rats [14; 15].

Tissue inflammation triggers multiple cytokine, chemokine and receptor-mediated events driving fibrogenesis. The GFP+/F4/80+ macrophages/monocytes and GFP+/vimentin+ mesenchymal cells in *Atp7b-/-* mice after BMT should have contributed to inflammatory cytokines and fibrogenesis. Inflammatory cytokines and chemokines, including *TNFα* and *IL6*, from activated neutrophils and KC impair hepatocyte survival and liver repopulation [32; 33]. Previous studies of hepatic stellate cells (HSC) indicated these play important roles in ECM remodeling during cell engraftment in liver [34]. HSC release deleterious cytokines during fibrogenesis, e.g., *TGFβ*, to suppress hepatocyte proliferation [35]. This might have affected proliferation in donor-derived cells in WD. Activation of HSC promotes expansion of myofibroblasts, which was reproduced by donor BM-derived cells in hepatic fibrosis [36]. Similarly, exposure of transplanted HSC to fibrogenic injuries in the liver led to their conversion into myofibroblasts, along with recruitment of monocytes and KC to further exacerbate hepatic fibrosis [37]. Targeting of donor-derived myofibroblasts involves ligand-receptor interactions, e.g., cannabinoid receptors [38]. Altered expression of

matrix degrading enzymes (*MMP*, *TIMP*) and of collagen in *Atp7b-/-* mice after BMT was in agreement with contribution of inflammatory cell types in hepatic fibrosis.

Stem cell transplantation is of interest for chronic liver disease [7], although trials of hematopoietic or mesenchymal stem cells (MSC) have not shown clear benefits [39]. In one animal study, BM-derived healthy MSC expressing *Atp7b* [40], improved their survival and proliferation. In another study, transplantation of *Atp7b*-transduced MSC in LEC rats [41], decreased liver Cu over the short-term. Our work in *Atp7b*-/- mice indicates analysis of candidate stem cells in representative settings will be helpful for clinical trials.

Acknowledgements

Supported in part by NIH grants R01-DK071111, P30-DK41296, P30-CA013330 and P30 DK020541, and by New York State Department of Health / NYSTEM Shared Facilities program, contract C029154. Gertrude Ukpong contributed technical expertise.

REFERENCES

1. Viswanathan P, Gupta P, Kapoor S, Gupta S. 2016. Thalidomide promotes transplanted cell engraftment in the rat liver by modulating inflammation and endothelial integrity. J Hepatol. 65(6):1171-1178.
2. Yovchev MI, Xue Y, Shafritz DA, Locker J, Oertel M. 2014. Repopulation of the fibrotic/cirrhotic rat liver by transplanted hepatic stem/progenitor cells and mature hepatocytes. Hepatology. 59(1):284-295.
3. Lagasse E, Connors H, Al-Dhalimy M, Reitsma M, Dohse M, Osborne L, Wang X, Finegold M, Weissman IL, Grompe M. 2000. Purified hematopoietic stem cells can differentiate into hepatocytes in vivo. Nat Med. 6(11):1229-1234.
4. Grompe M, Strom S. 2013. Mice with human livers. Gastroenterology. 145(6):1209-1214.
5. Roobrouck VD, Clavel C, Jacobs SA, Ulloa-Montoya F, Crippa S, Sohni A, Roberts SJ, Luyten FP, Van Gool SW, Sampaolesi M et al. 2011. Differentiation potential of human postnatal mesenchymal stem cells, mesoangioblasts, and multipotent adult progenitor cells reflected in their transcriptome and partially influenced by the culture conditions. Stem Cells. 29(5):871-882.
6. Espejel S, Eckardt S, Harbell J, Roll GR, McLaughlin KJ, Willenbring H. 2014. Brief report: Parthenogenetic embryonic stem cells are an effective cell source for therapeutic liver repopulation. Stem Cells. 32(7):1983-1988.
7. Forbes SJ, Gupta S, Dhawan A. 2015. Cell therapy for liver disease: From liver transplantation to cell factory. J Hepatol. 62(1 Suppl):S157-169.
8. Zhu S, Rezvani M, Harbell J, Mattis AN, Wolfe AR, Benet LZ, Willenbring H, Ding S. 2014. Mouse liver repopulation with hepatocytes generated from human fibroblasts. Nature. 508(7494):93-97.
9. Bandi S, Cheng K, Joseph B, Gupta S. 2012. Spontaneous origin from human embryonic stem cells of liver cells displaying conjoint meso-endodermal phenotype with hepatic functions. J Cell Sci. 125(Pt 5):1274-1283.
10. Gupta S, Rajvanshi P, Lee CD. 1995. Integration of transplanted hepatocytes into host liver plates demonstrated with dipeptidyl peptidase iv-deficient rats. Proc Natl Acad Sci U S A. 92(13):5860-5864.
11. Gupta S, Rajvanshi P, Sokhi R, Slehria S, Yam A, Kerr A, Novikoff PM. 1999. Entry and integration of transplanted hepatocytes in rat liver plates occur by disruption of hepatic sinusoidal endothelium. Hepatology. 29(2):509-519.
12. Baligar P, Kochat V, Arindkar SK, Equbal Z, Mukherjee S, Patel S, Nagarajan P, Mohanty S, Teckman JH, Mukhopadhyay A. 2017. Bone marrow stem cell therapy partially ameliorates pathological consequences in livers of mice expressing mutant human alpha1-antitrypsin. Hepatology. 65(4):1319-1335.
13. Schilsky ML. 2014. A century for progress in the diagnosis of wilson disease. J Trace Elem Med Biol. 28(4):492-494.
14. Malhi H, Joseph B, Schilsky ML, Gupta S. 2008. Development of cell therapy strategies to overcome copper toxicity in the lec rat model of wilson disease. Regen Med. 3(2):165-173.

15. Joseph B, Kapoor S, Schilsky ML, Gupta S. 2009. Bile salt-induced pro-oxidant liver damage promotes transplanted cell proliferation for correcting wilson disease in the long-evans cinnamon rat model. Hepatology. 49(5):1616-1624.
16. Murillo O, Luqui DM, Gazquez C, Martinez-Espartosa D, Navarro-Blasco I, Monreal JI, Guembe L, Moreno-Cermeno A, Corrales FJ, Prieto J et al. 2016. Long-term metabolic correction of wilson's disease in a murine model by gene therapy. J Hepatol. 64(2):419-426.
17. Gupta S. 2014. Cell therapy to remove excess copper in wilson's disease. Ann N Y Acad Sci. 1315:70-80.
18. Lutsenko S. 2008. Atp7b-/- mice as a model for studies of wilson's disease. Biochem Soc Trans. 36(Pt 6):1233-1238.
19. Merlin S, Bhargava KK, Ranaldo G, Zanolini D, Palestro CJ, Santambrogio L, Prat M, Follenzi A, Gupta S. 2016. Kupffer cell transplantation in mice for elucidating monocyte/macrophage biology and for potential in cell or gene therapy. Am J Pathol. 186(3):539-551.
20. Follenzi A, Raut S, Merlin S, Sarkar R, Gupta S. 2012. Role of bone marrow transplantation for correcting hemophilia a in mice. Blood. 119(23):5532-5542.
21. Jaber FL, Sharma Y, Gupta S. 2017. Demonstrating potential of cell therapy for wilson's disease with the long-evans cinnamon rat model. Methods in molecular biology (Clifton, NJ). 1506:161-178.
22. Malhi H, Bhargava KK, Afriyie MO, Volenberg I, Schilsky ML, Palestro CJ, Gupta S. 2002. 99mtc-mebrofenin scintigraphy for evaluating liver disease in a rat model of wilson's disease. J Nucl Med. 43(2):246-252.
23. Evenson MA. 1988. Measurement of copper in biological samples by flame or electrothermal atomic absorption spectrometry. Methods Enzymol. 158:351-357.
24. Gorla GR, Malhi H, Gupta S. 2001. Polyploidy associated with oxidative injury attenuates proliferative potential of cells. J Cell Sci. 114(Pt 16):2943-2951.
25. Travis EL, Peters LJ, McNeill J, Thames HD, Jr., Karolis C. 1985. Effect of dose-rate on total body irradiation: Lethality and pathologic findings. Radiotherapy and oncology : journal of the European Society for Therapeutic Radiology and Oncology. 4(4):341-351.
26. Qiao J, Fu J, Fang T, Huang Y, Mi H, Yang N, Chen C, Xu K, Zeng L. 2015. Evaluation of the effects of preconditioning regimens on hepatic veno-occlusive disease in mice after hematopoietic stem cell transplantation. Exp Mol Pathol. 98(1):73-78.
27. Bandi S, Gupta S, Tchaikovskaya T, Gupta S. 2018. Differentiation in stem/progenitor cells along fetal or adult hepatic stages requires transcriptional regulators independently of oscillations in microrna expression. Exp Cell Res.
28. Allen KJ, Cheah DM, Lee XL, Pettigrew-Buck NE, Vadolas J, Mercer JF, Ioannou PA, Williamson R. 2004. The potential of bone marrow stem cells to correct liver dysfunction in a mouse model of wilson's disease. Cell Transplant. 13(7):765-773.
29. Vogel A, Aslan JE, Willenbring H, Klein C, Finegold M, Mount H, Thomas G, Grompe M. 2006. Sustained phosphorylation of bid is a marker for resistance to fas-induced apoptosis during chronic liver diseases. Gastroenterology. 130(1):104-119.

30. Vassilopoulos G, Wang PR, Russell DW. 2003. Transplanted bone marrow regenerates liver by cell fusion. Nature. 422(6934):901-904.
31. Giri RK, Malhi H, Joseph B, Kandimalla J, Gupta S. 2003. Metal-catalyzed oxidation of extracellular matrix components perturbs hepatocyte survival with activation of intracellular signaling pathways. Exp Cell Res. 291(2):451-462.
32. Krohn N, Kapoor S, Enami Y, Follenzi A, Bandi S, Joseph B, Gupta S. 2009. Hepatocyte transplantation-induced liver inflammation is driven by cytokines-chemokines associated with neutrophils and kupffer cells. Gastroenterology. 136(5):1806-1817.
33. Viswanathan P, Kapoor S, Kumaran V, Joseph B, Gupta S. 2014. Etanercept blocks inflammatory responses orchestrated by tnf-alpha to promote transplanted cell engraftment and proliferation in rat liver. Hepatology. 60(4):1378-1388.
34. Benten D, Kumaran V, Joseph B, Schattenberg J, Popov Y, Schuppan D, Gupta S. 2005. Hepatocyte transplantation activates hepatic stellate cells with beneficial modulation of cell engraftment in the rat. Hepatology. 42(5):1072-1081.
35. Dixon M, Agius L, Yeaman SJ, Day CP. 1999. Inhibition of rat hepatocyte proliferation by transforming growth factor beta and glucagon is associated with inhibition of erk2 and p70 s6 kinase. Hepatology. 29(5):1418-1424.
36. Forbes SJ, Russo FP, Rey V, Burra P, Rugge M, Wright NA, Alison MR. 2004. A significant proportion of myofibroblasts are of bone marrow origin in human liver fibrosis. Gastroenterology. 126(4):955-963.
37. Benten D KJ, Wirth JW, Thiele ND, Follenzi A, Bhargava KK, Palestro CJ, Koepke M, Tjandra R, Volz T, Lutgehetmann M, Gupta S. 2018. A humanized mouse model with liver fibrosis following expansion of transplanted hepatic stellate cells in injury and inflammation. Laboratory investigation; a journal of technical methods and pathology.In press.
38. Wang L, Yang L, Tian L, Mai P, Jia S, Yang L, Li L. 2017. Cannabinoid receptor 1 mediates homing of bone marrow-derived mesenchymal stem cells triggered by chronic liver injury. J Cell Physiol. 232(1):110-121.
39. Nicolas CT, Wang Y, Nyberg SL. 2016. Cell therapy in chronic liver disease. Curr Opin Gastroenterol. 32(3):189-194.
40. Sauer V, Siaj R, Todorov T, Zibert A, Schmidt HH. 2010. Overexpressed atp7b protects mesenchymal stem cells from toxic copper. Biochem Biophys Res Commun. 395(3):307-311.
41. Chen S, Shao C, Dong T, Chai H, Xiong X, Sun D, Zhang L, Yu Y, Wang P, Cheng F. 2014. Transplantation of atp7b-transduced bone marrow mesenchymal stem cells decreases copper overload in rats. PLoS One. 9(11):e111425.

Table 1

RT-PCR primers

Gene (NCBI ID)	Primers	Amplicon Size	Tm (ºC)
Tgfβ1 (21803)	Forward: 5'-CTCCCGTGGCTTCTAGTGC-3' Reverse: 5'-GCCTTAGTTTGGACAGGATCTG-3'	133	60
Collagen type 1 (12842)	Forward: 5'-GCTCCTCTTAGGGGCCACT-3' Reverse: 5'-CCACGTCTCACCATTGGGG-3'	103	60
Timp1 (21857)	Forward: 5'-CGAGACCACCTTATACCAGCG-3' Reverse: 5'-ATGACTGGGGTGTAGGCGTA-3'	108	60
Mmp2 (17390)	Forward: 5'-ACCTGAACACTTTCTATGGCTG-3' Reverse: 5'-CTTCCGCATGGTCTCGATG-3'	140	60
Tnf (21926)	Forward: 5'-CAGGCGGTGCCTATGTCTC-3' Reverse: 5'-CGATCACCCCGAAGTTCAGTAG-3'	89	60
Il6 (16193)	Forward: 5'-TCTATACCACTTCACAAGTCGGA-3' Reverse: 5'-GAATTGCCATTGCACAACTCTTT-3'	88	60
Atp7b (11979)	Forward: 5'-GGGGACGATGCCTGAACAG-3' Reverse, 5'-TAGCCAACATTGTCGAAGGCG-3'	135	60
Gapdh (2597)	Forward: 5'-GGCCTCCAAGGAGTAAGACC-3' Reverse: 5'-AGGGGTCTACATGGCAACTG-3'	127	60

Table 2

Morphometry for donor-derived cells in liver of *Atp7b-/-* mice 1 year after BMT*

Donor-derived cell type	Number GFP+ donor BM cells per high power field, means ± SEM (n)*	Number GFP+ / hepatic marker+ donor BM-derived cells per high power field*	Percent of GFP+ cells (mean)	P values (ANOVA)**
Hepatocytes with DPPIV+ bile canaliculi	136 ± 2 (n=61)	0.05 ± 0.0	0.04	-
F4/80+ Kupffer cells and monocytes	142 ± 2 (n=40)	20 ± 1	14	<0.001
Vimentin+ mesenchymal cells	154 ± 2 (n=47)	129 ± 2	84	<0.001

*Cell numbers were multiplied by factor of 2 because 50% of GFP+/- transgenic donor cells expressed GFP

**p values versus percent of GFP+ hepatocytes

FIGURE LEGENDS

Fig. 1. Animal outcomes after BMT. (A) Experimental plan and timeline, including animal groups, and end-points over 12 mo study period. **(B)** GFP expression in hepatocytes and other cell types in donor liver (top left panel; inset, GFP+ cell in hepatic sinusoid, arrow). GFP was absent in C57BL/6 or Atp7b-/- controls (top middle panel). Transplanted GFP+ hepatocytes after 3 mo in *Atp7b-/-* mice forming expanding cluster (arrow, top right panel, DAB color development). GFP+ donor-derived cells in *Atp7b-/-* mice 3 mo after BMT (inset in panel at bottom left: arrow, GFP+ hepatocyte). GFP and bile canalicular Dpp4 (red) in *Atp7b-/-* mouse 3 mo after BMT (magnified view of boxed area: arrow, GFP+/Dpp4+ hepatocyte; arrowhead, Dpp4+ sinusoidal cell). Original magnification: top panels x600; bottom panels, x400. DAPI counterstain. (**C**) Serum ALT levels were elevated in *Atp7b*-/- mice and increased after BMT. (**D**) Serum ceruloplasmin was lower in *Atp7b*-/- mice with or without BMT than healthy controls. P values, ANOVA, Kruskall-Wallis test.

Fig. 2. Liver histology after 12 mo. (A) Healthy C57/BL6 mice showed normal morphology (left, inset, arrow, size of normal nuclei). Liver injury was evident in *Atp7b-/-* mice, including after BMT (insets, megalocytes with enlarged nuclei). **(B)** Sirius Red staining showed more collagen in untreated *Atp7b-/-* controls and *Atp7b-/-* mice after BMT. Original magnification, x400. **(C)** Grading for tissue histology indicated worsening in *Atp7b-/-* mice after BMT. **(D)** Tissue hydroxyproline levels were higher in *Atp7b*-/- mice than healthy controls. These increased in mice after BMT. P values, ANOVA with Kruskall-Wallis test.

Fig. 3. Hepatic Cu and *Atp7b* mRNA with changes in liver cells. (A) Compared with healthy C57BL/6 mice liver Cu content increased in *Atp7b-/-* controls and *Atp7b-/-* mice after BMT. **(B)** RT-PCR revealed *Atp7b* mRNA in healthy C57BL/6 mice but in neither untreated *Atp7b-/-* mice nor *Atp7b-/-* mice after BMT. (**C**) Oxidative DNA damage with 8-oxo-dG adducts in liver (red color) in *Atp7b-/-* mice after 12 mo, including in hepatocytes and inflammatory or stromal cells. These adducts were abundant in *Atp7b-/-* mice after BMT. Chart provides cumulative analysis for adducts. Original magnification, x400. DAPI counterstain.

Fig. 4. Quantitative RT-PCR for inflammatory and fibrogenic genes. Gene expression normalized to Gapdh in C57BL/6 and *Atp7b-/-* control mice and *Atp7b-/-* mice 6 mo or 12 mo after BMT. *IL6* and *TNF-α* were expressed more after BMT. Similarly**,** *TGF-β*, *TIMP1* and collagen1 were expressed more, but *MMP2* was expressed less after BMT, indicating fibrogenesis-associated processes. These changes were more pronounced at 6 mo after BMT. Whether more fibrosis at later times introduced sampling issues was not excluded. P values, ANOVA with Kruskall-Wallis test.

Fig. 5. Donor BM-derived cell types in liver after 12 mo. **(A)** GFP and Dpp4 staining for bile canaliculi (red color) in hepatocytes. GFP+/Dpp4+ cells did not expand or form clusters after BMT. **(B)** F4/80 (red) in donor-derived monocytes/macrophages (inset, arrow, GFP+/F4/80+ cell in sinusoid). **(C)** Costaining for vimentin (red) with green/yellow donor-derived myofibroblasts throughout liver (inset, arrow, donor-derived myofibroblast). Original magnification, x400. DAPI counterstain.

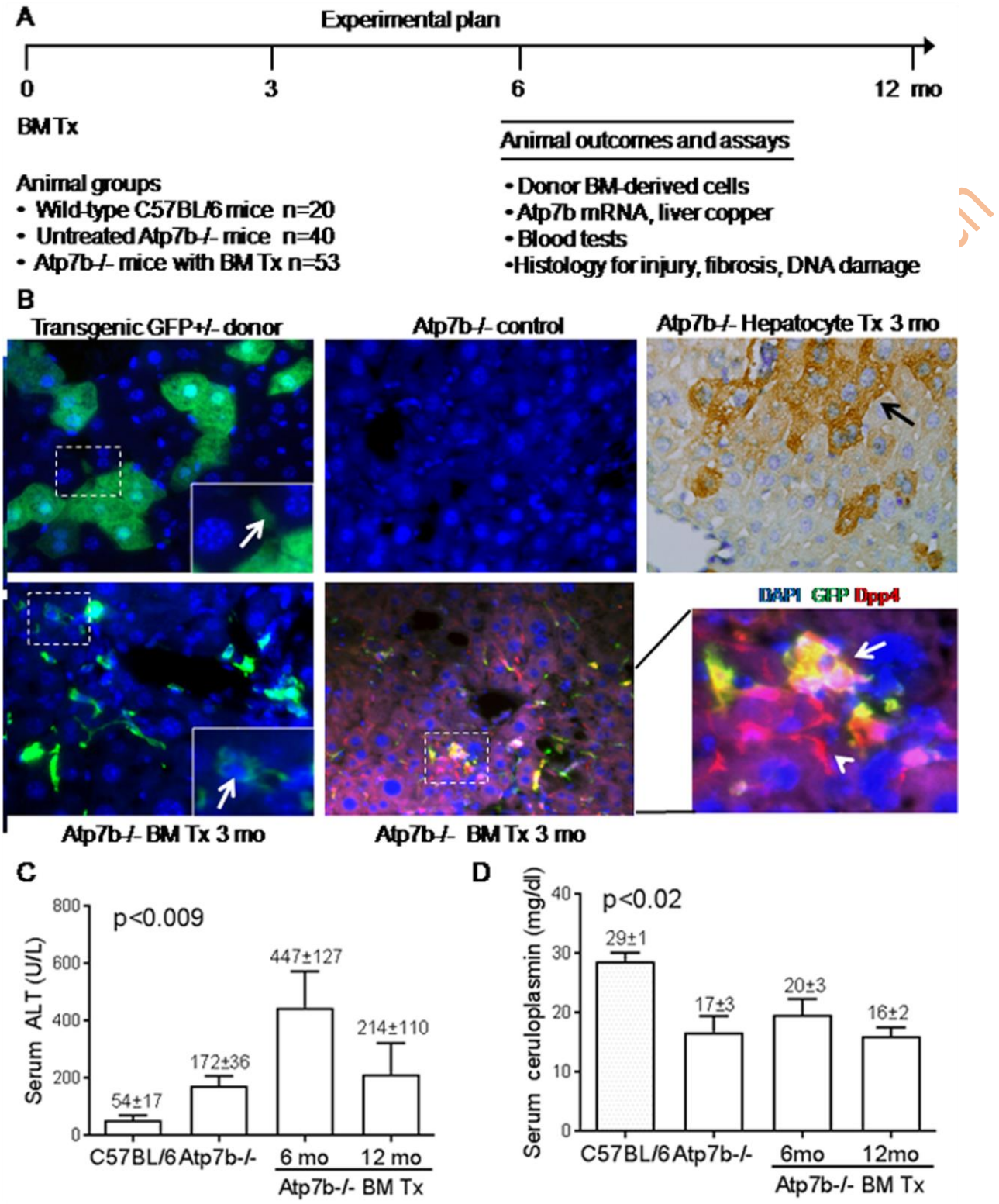

Figure 1

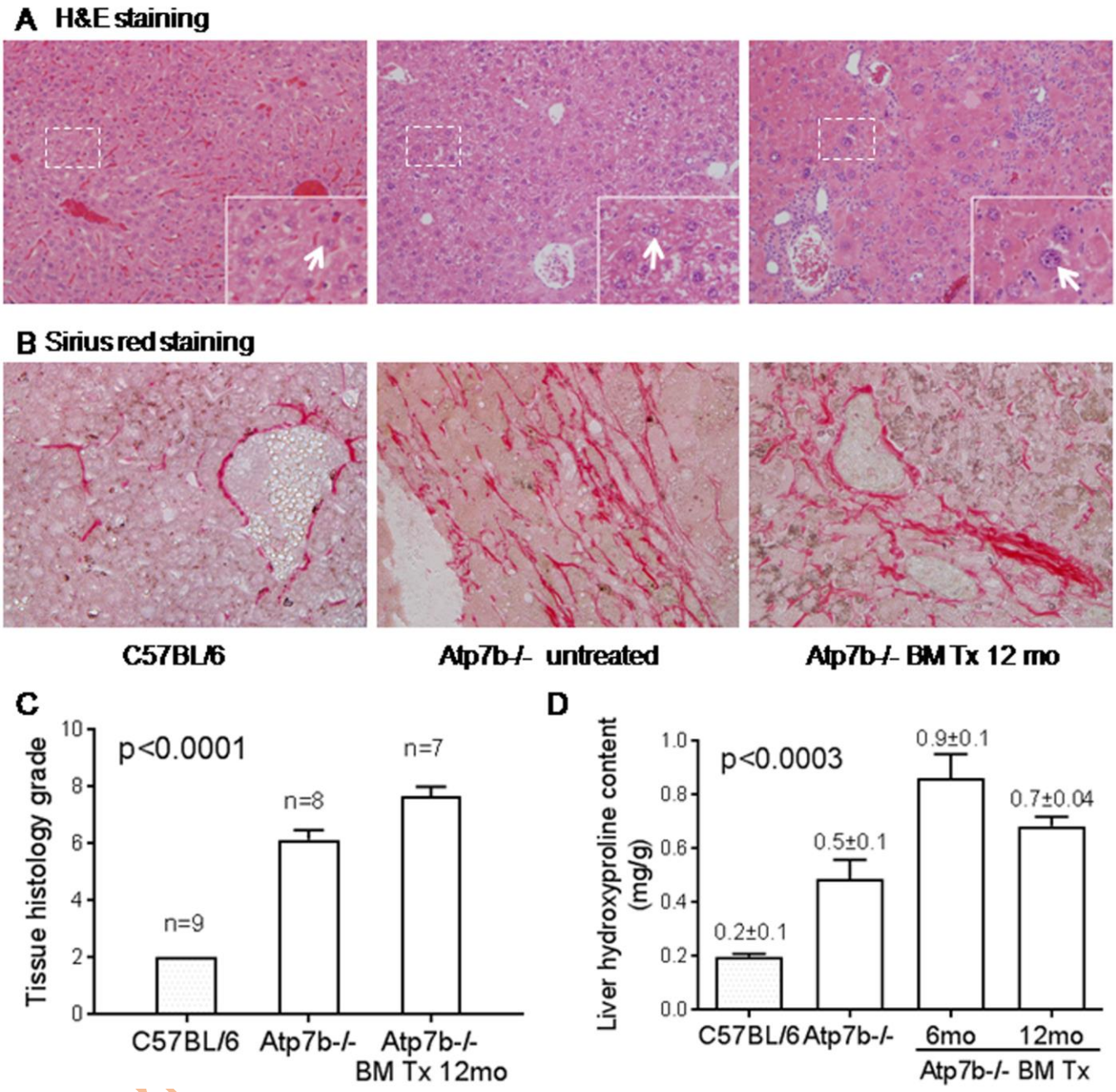

Figure 2

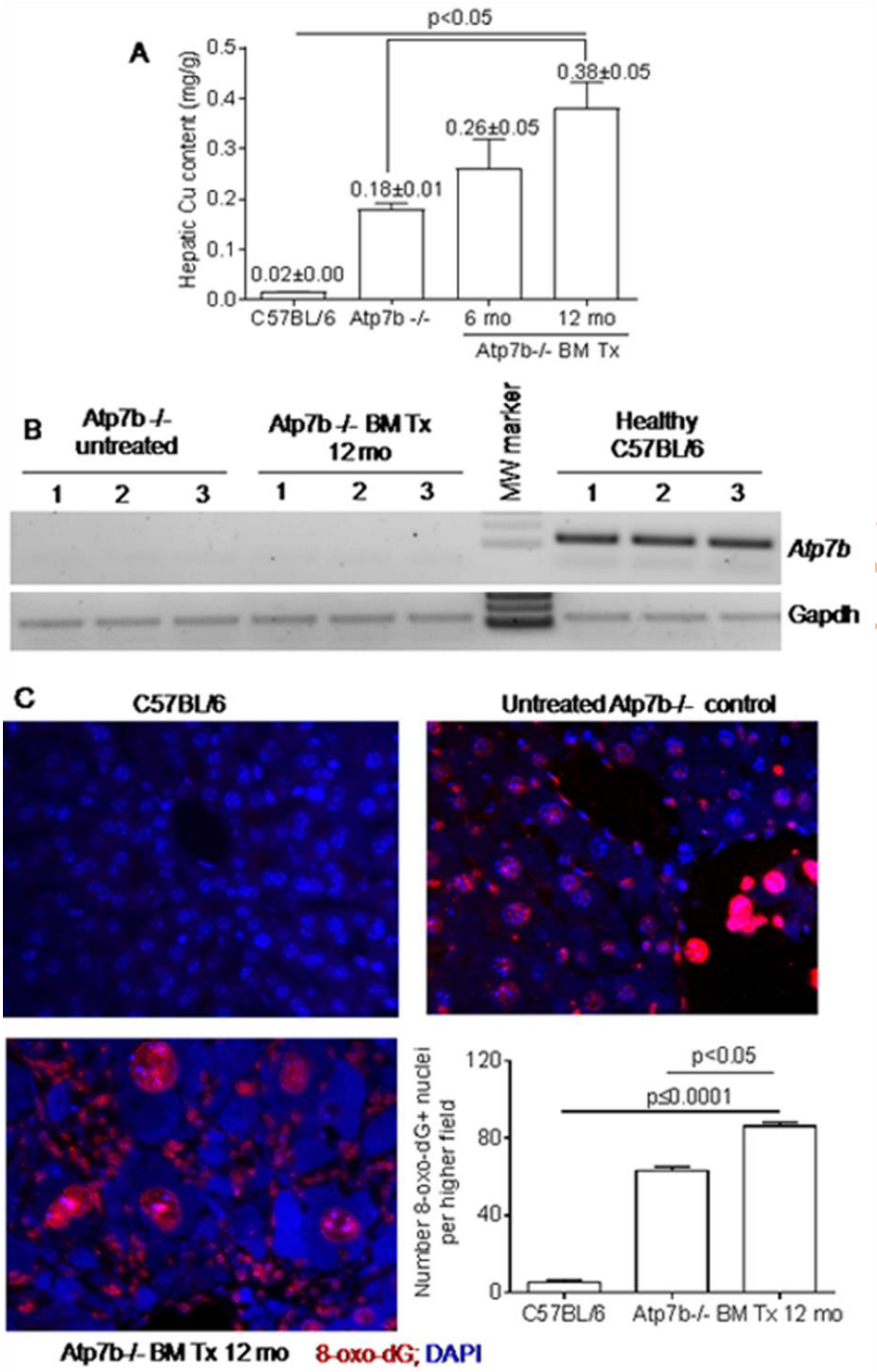

Figure 3

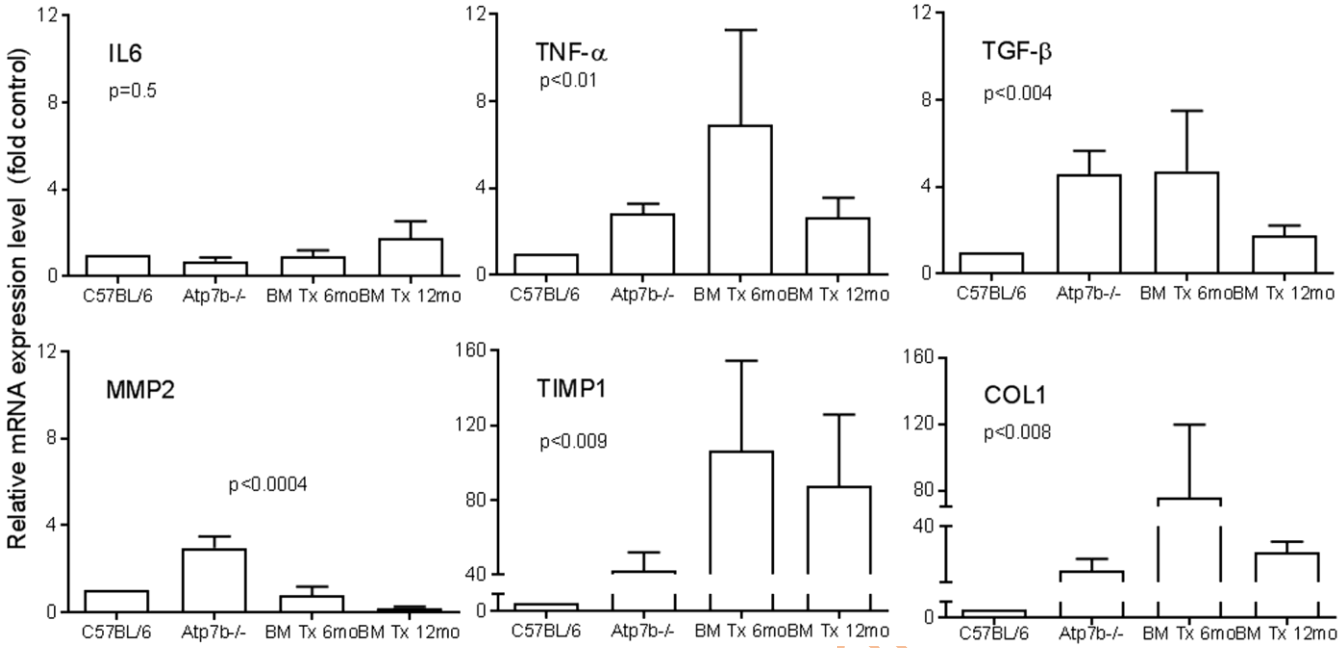

Figure 4

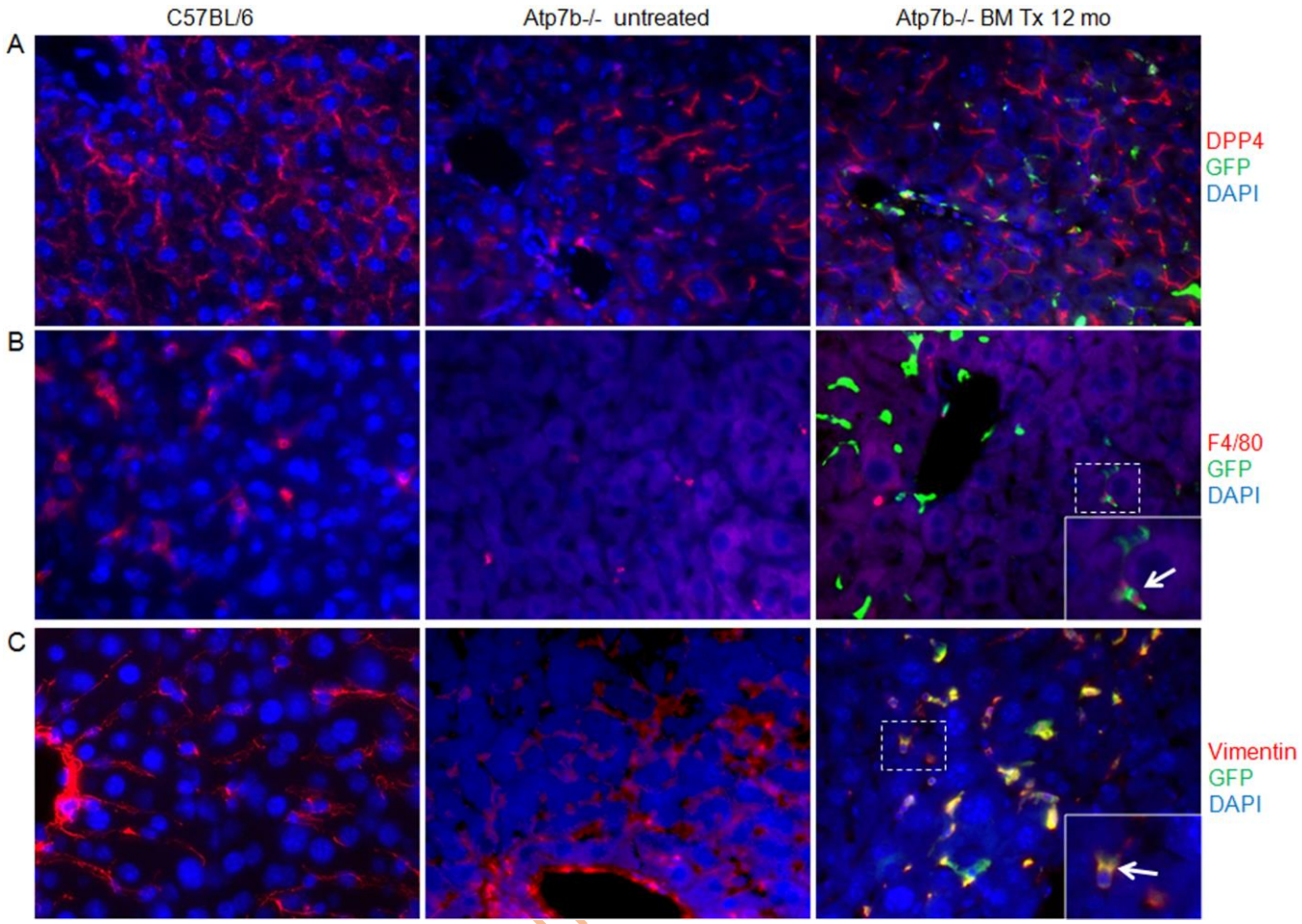

Figure 5